

Structural and Morphological Properties of Spinel Type Magnesium Aluminate Thick Films

T.R.TATTE

Department of Physics, Shri. Dr. R. G. Rathod Arts and Science College, Murtizapur, Dist. Akola, Maharashtra State, India

Abstract- Magnesium aluminate ($MgAl_2O_4$) powder sample was successfully prepared by co-precipitation method. The structural properties of the prepared material was investigated by X-ray diffraction (XRD) and Fourier transform infrared spectroscopy (FTIR). XRD study shows that the sample has the spinel structure and crystallite size of the prepared sample was 6.2 nm. FTIR spectrum explained the vibrational stretching frequencies of the material. Results of transmission electron microscopy with electron diffraction (TEM-ED) corroborates with XRD analysis. The morphology of the film and elemental composition of the sample was studied by using scanning electron microscopy with energy dispersive X-ray analysis (SEM-EDAX) and the result shows the prepared film contain highly porous structure.

Indexed Terms- Magnesium aluminate, XRD, FT-IR, SEM, TEM

I. INTRODUCTION

The environment contains a mixture of synthetically produced chemical components, toxic and explosive gases. Monitoring is needed so that effective measures can be taken to control and minimize the emission of hazardous gases to keep the environment safe and clean. At present, there are large number of gas detecting systems that have been used in process, for high performance gas sensors with high sensitivity and selectivity [1, 2]. Semiconductor gas sensor is chemiresistive type gas sensor. Chemiresistive gas sensors are based on SnO_2 , TiO_2 , WO_3 , NiO , ZnO , Al_2O_3 , CuO , In_2O_3 , Cr_2O_3 , etc. metal oxide material.

These materials can be utilized to detect combustible, reducing, or oxidizing gases with sensors which are based on the resistance change responses to the target gases [3]. The SMO sensor detecting harmful gases

like CO, H_2S , H_2 , NO_x and hydrocarbons (propane, butane etc.) low concentration level because of their high sensitivity, robustness and simple signal processing. Nanocrystalline structured gas sensing materials have been developed to enhance the sensitivity of a SMO sensor. The magnesium aluminate spinel possesses the properties such as high resistance to chemical attack, good mechanical strength from room temperature to high temperatures, low dielectric constant, excellent optical properties, low thermal expansion and good catalytic properties [4-8].

Moreover, there are different methods available to achieve nanocrystalline metal oxides with small particle size, such as combustion, hydrothermal route [9-13], citrated sol-gel method, Sono-chemical method, microwave heating, polymer solution route, solid state reaction method [14], co-precipitation [15,16] and self-heat sustained technique.

Among these methods, co-precipitation method is very easy and low cost method, which is operated at low temperature. Moreover, considering the importance of $MgAl_2O_4$ in various applications, it was decided to study magnesium aluminate prepared by co-precipitation method and to evaluate their structural properties.

II. EXPERIMENTAL

Magnesium aluminate ($MgAl_2O_4$) has been prepared by co-precipitation route. High purity precursors were used for the synthesis of the powder. As a result no further refinement was needed. Aluminum nitrate [$Al(NO_3)_3 \cdot 9H_2O$], magnesium nitrate [$Mg(NO_3)_2 \cdot 6H_2O$] and ammonia solution (25 wt. %) Sd fine GR grade chemical are used for the synthesis of nanoparticles.

In the beginning, the stoichiometric molar amounts of analytically pure [$Al(NO_3)_3 \cdot 9H_2O$] and

[Mg(NO₃)₂·6H₂O] were weighed and dissolved in distilled water and subsequently stirred at 80°C for 2 h to obtain a homogeneous and stable solution. Then aqueous ammonia (25 wt. %) was added drop wise at room temperature in the resulting liquid mixture under vigorous stirring till pH becomes 9. Here ratio of Mg/Al is 1:2. The collected precipitates comprising of hydroxides of metal ions and some water contents [17]. This precipitate was filtered-washed with ethanol and distilled water for number of times to remove excess of ammonia. In second stage, resulting precipitate was dried in oven for 22 h at 110°C to evaporate the water content. Calcination was done at 800°C for 4 h in furnace to obtain MgAl₂O₄. Taken solid phase sample was grinded in a mortar to make it powder.

The synthesized powder and a solution of ethyl cellulose (a temporary binder) were mixed together with butylcellulose, butyl carbitol acetate and turpeneol in order to obtain the paste. Pastes incorporating mass percentage ratio of 80:20, with MgAl₂O₄ and the binder respectively were ground in an agate pestle and mortar with for 1 h. This paste was screen printed onto glass substrate surface in desired patterns. This thick film was allowed to dry for 24 h at room temperature and heat treatment was given to the film at 500°C for 1 h.

III. RESULT AND DISCUSSIONS

3.1 XRD Analysis

Figure 1 depicts the XRD pattern of MgAl₂O₄ powder prepared by co-precipitation method. XRD pattern shows the spinel structure in accordance with JCPDS card. No other phases were detected in the calcinated sample. For MgAl₂O₄, the characteristic peaks for spinel structure were broad with maximum at 18.71, 30.89, 36.37, 44.51, 59.02, 64.99, 77.05 and 82.41 which can be indexed as (1 1 1), (2 2 0), (3 1 1), (4 0 0), (5 1 1), (4 4 0), (5 3 3) and (4 4 4) diffraction planes, respectively. The crystallite size has been calculated from the XRD peaks using Debye-Scherrer formula. Further, the lattice parameter of the prepared powder was calculated from the XRD peaks by indexing corresponding peaks in a cubic space group Fd-3m, using least square refinement. The XRD pattern show the formation of crystalline cubic structure.

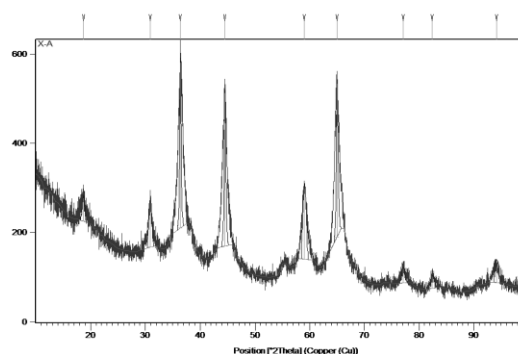


Figure 1: X-ray diffraction pattern of MgAl₂O₄ powder calcinated at 800°C.

3.2 FT-IR Analysis

Figure 2 shows the FT-IR spectrum of the MgAl₂O₄ nanoparticle. The peak position at 3457.05 cm⁻¹ was attributed to the O-H stretching vibration and 1642.67 cm⁻¹ which is due to the moisture adsorbed by the product [18-22]. From Figure 2, it can be observed that the peak at 1518.25 cm⁻¹ was attributed to Al-O stretching vibration [23]. The splitting of the high frequency band may be explained by the statement that a certain number of Al³⁺ ions occupy the tetrahedral site in the spinel structure [24]. The sample measurement of spectrum shows the bands which are in almost good conformity with ideal values of single crystals. The changes in the observed values are due to the formation of nanophase. The bands appeared at 527.98 assigned to the spinel formation of MgAl₂O₄.

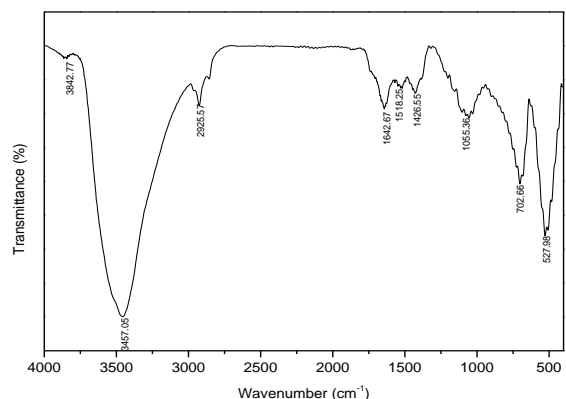


Figure 2: FT-IR spectrum of MgAl₂O₄ powder calcinated at 800°C.

3.3 SEM Analysis

The surface morphology of thick film was analyzed by using scanning electron microscope (SEM). SEM image of MgAl_2O_4 thick film is shown in Figure 3. SEM image show a few particles are in the range 24-26 nm and some agglomerates are formed. The microstructure shows the homogeneous distribution of the particles in the sample. The film contains highly porous structure which has a large portion of atoms residing at surfaces and interfaces between the pores.

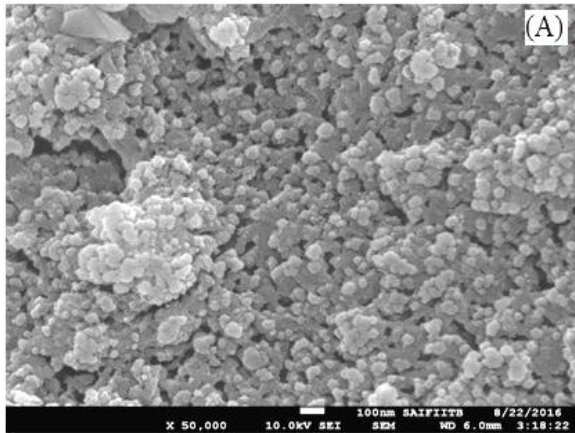


Figure 3: SEM image of nanocrystalline MgAl_2O_4

3.4 EDAX

Figure 4 shows the EDAX spectrum of MgAl_2O_4 thick film. The elemental analysis as obtained from EDAX is in close agreement with the starting composition used for the synthesis. Spectrum reveals presence of Mg, Al, and O elements.

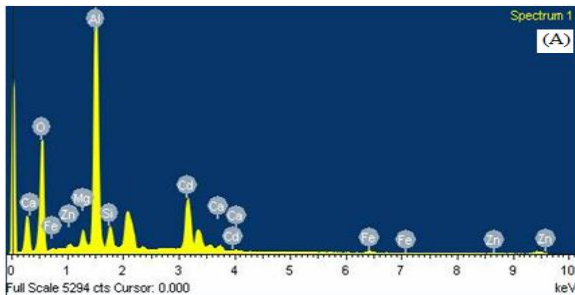


Figure 4: EDAX spectrum of MgAl_2O_4

3.5 TEM

Morphology of MgAl_2O_4 was characterized with Transmission Electron Microscopy (TEM). TEM image of MgAl_2O_4 powder annealed at 800°C is shown in Figure 5. Figure exhibits the local distribution of the crystallite size can be revealed.

The average crystallite size calculated from the XRD data agrees with the TEM results. The small amount of agglomerations is observed in the micrograph.

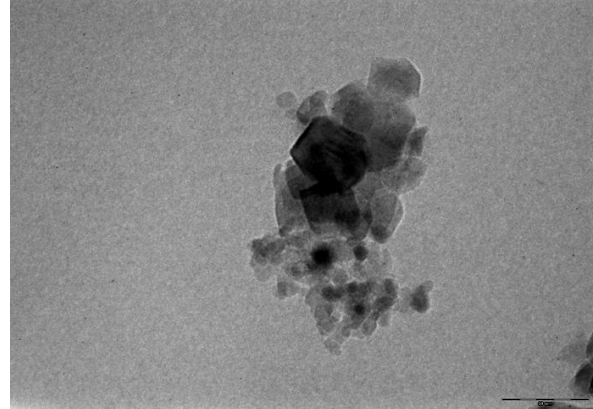


Figure 5: TEM photograph of MgAl_2O_4 .

3.6 SAED

The selected area electron diffraction (SAED) pattern is presented in Figure 6. From figure 6, it can be seen that there is presence of continuous rings which deduced that the orientation of the crystallites is random within the field of view. It is observed that the spottype pattern which is indicative of the presence of single crystallite particles and no evidence was found for more than onepattern, suggesting the single-phase nature of the material.

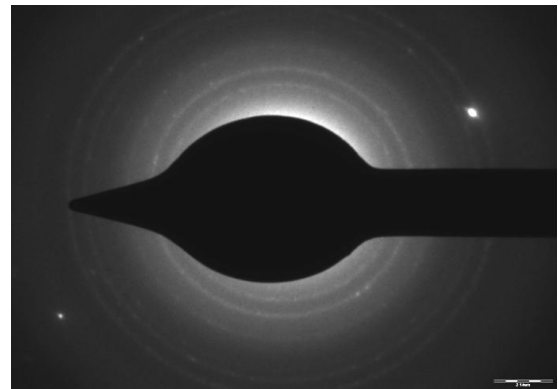


Figure 6: Selected area diffraction pattern of MgAl_2O_4 powder.

CONCLUSION

In the present study, MgAl_2O_4 powder sample was successfully prepared using less expensive, environment-friendly and low temperature co-precipitation route. XRD pattern reveals the formation of nanocrystalline cubic structure of prepared sample. The crystallite size is 6.2 nm. FT-IR

spectrum explained the vibrational stretching frequencies of the material. The decrease in intensity of the absorption band in FT-IR spectra suggested the occupation of ions at the octahedral B site. By using scanning electron microscopy with energy dispersive X-ray analysis (SEM-EDAX), the surface morphology and elemental composition of the sample was characterized. The average crystallite size of sample estimated from XRD analysis concurs with TEM investigation.

ACKNOWLEDGEMENT

The author thank to Sophisticated Analytical Instrument Facility (S.A.I.F.), Punjab University, Chandigarh for providing XRD facility. A special thanks to Indian Institute of Technology (IIT), Bombay for carrying out FT-IR, SEM-EDAX and TEM-ED characterizations.

REFERENCES

- [1] S. Zampolli, I. Elmi, F. Ahmed, M. Passini, G. C. Cardinali, S. Nicoletti, L. Dori, *Sens. and Actuat. B* 101 (2004) 39-46.
- [2] D. M. Bon, Ulbrich, I. M. Ulbrich, J. A. de Gouw, C. Warneke, W. C. Kuster, M. L. Alexander, A. Baker, A. J. Beyersdorf, D. Blake, R. Fall, *Chem. Phys.* 11 (2011) 2399-2421.
- [3] M. Batzill, U. Diebold, *Prog. Surf. Sci.* 79 (2005) 147-154.
- [4] G. B. Nuernberg, E. L. Foletto, C. Campos, H. Fajardob, N. Carreno, L. Probst, *J. Power Sour.* 208 (2012) 409-414.
- [5] F. Saito, W. Kim, *Powder Technol.* 113 (1999) 109-113.
- [6] T. W. Dung, L.R. Ping, A. M. Azad, *Mater. Res. Bull.* 36 (2001) 1417-1430.
- [7] A. D. Mazzoni, M. A. Sainz, A. Caballero, E. F. Aglietti, *Mater. Chem. Phys.* 78(2002)30-37.
- [8] S. A. Bocanegra, A. D. Ballarini, O. A. Scelza, S. R. Miguel, *Mater. Chem. Phys.* 111 (2008) 534-541.
- [9] D. Makovec, M. Drogenik, A. Znidarsic, *J. Eur. Ceram. Soc.* 21(2001) 1945-1949.
- [10] J. A. Toledo, M. A. Valenzuela, P. Bosch, *Appl. Catal. A.* 198 (2000) 235-245.
- [11] S. C. Goh, C. H. Chia, S. Zakaria, M. Yusoff, C. Y. Haw, Sh. Ahmadi, N. M. Huang, H. N. Lim, *Mater. Chem. Phys.* 120 (2010) 31-35.
- [12] D. Zhao, X. Wu, H. Guan, E. Han, *J. of Supercrit. Fluids* 42 (2007) 226-233.
- [13] Q. Liu, J. Sun, H. Long, X. Sun, X. Zhong, Z. Xu, *Mater. Chem. Phys.* 108 (2008) 269-273.
- [14] C. H. Yan, Z. G. Xu, F. X. Cheng, *Solid State Commun.* 111(1999) 287-291.
- [15] S. Toshihiko, I. Shinichiro, K. Takayuki, Y. Goro, *Int. J. Miner. Process.* 62 (2001) 94-95.
- [16] K. Kaneko, T. Katsura, *Bull. Chem. Soc. Jpn.* 52 (1979) 96-100.
- [17] Z. Yue, W. Guo, J. Zhou, Z. Gui, L. Li, *J. Magn. Mater.* 270 (2004) 216-233.
- [18] K. Nakamoto, *Organometallic, and Bioinorganic Chemistry*, sixth ed., Wiley-Interscience, USA, 2009.
- [19] M.Y. Nassar, A. S. Attia, K. A. Alfallous, M. F. El-Shahat, *Inorg. Chim. Acta* 405 (2013) 362-367.
- [20] M.Y. Nassar, *Mater. Lett.* 94 (2013) 112-115.
- [21] M.Y. Nassar, I. S. Ahmed, *Mater. Res. Bull.* 47 (2012) 2638-2645.
- [22] M.Y. Nassar, I. S. Ahmed, *Polyhedron* 30 (2011) 2431-2437.
- [23] G. Korotcenkov, I. Boris, A. Cornet, J. Rodriguez, A. Cirera, V. Golovanov, Y. Lychkovsky, G. Karkotsky, *Sens. and Actuat. B* 120 (2007) 657-664.
- [24] B. L. Patil, S. R. Sawant, S. A. Patil, *J. Matter Sci.* 29(1994) 175-178.